

The Absorption Spectrum of Europium

G. Smith and F. S. Tomkins

Phil. Trans. R. Soc. Lond. A 1976 **283**, 345-365

doi: 10.1098/rsta.1976.0089

Email alerting service

Receive free email alerts when new articles cite this article - sign up in the box at the top right-hand corner of the article or click [here](#)

THE ABSORPTION SPECTRUM OF EUROPIUM

BY G. SMITH

Department of Astrophysics, Oxford University, England

AND F. S. TOMKINS

*Argonne National Laboratory, Argonne, Illinois, U.S.A.**(Communicated by W. R. S. Garton, F.R.S. – Received 23 February 1976)*

[Plate 1]

CONTENTS

	PAGE		PAGE
1. INTRODUCTION	345	(b) $4f^7 (^8S) 5d 6p$	356
2. EXPERIMENTAL	346	(c) $4f^7 (^8S) 6s 7p$	357
		(d) $4f^6 (^7F) 5d 6s^2$	357
3. RESULTS	347	(e) $4f^6 (^7F) 5d^2 6s$	358
(a) Wavelengths, intensities and upper energy levels	354	(f) $4f^6 (^7F) 5d^3$	359
(b) J -values and g_J -values	354	(g) Levels based on excited parent terms of $4f^7$	359
(c) Isotope shifts	355	5. LONG SERIES	359
4. CONFIGURATION STRUCTURE	356	6. CONCLUSION	364
(a) $4f^7 (^8S) 6s 6p$	356	REFERENCES	365

The europium absorption spectrum has been photographed at high resolution in the spectral region 7200–2100 Å which includes the entire sharp-line spectrum longward of the first ionization limit. Wavelengths and wavenumbers have been determined by comparison with thorium standards. Since all transitions take place from the ground level the wavenumbers correspond to excitation energies of even-parity levels with total angular momentum (J) of $\frac{5}{2}$, $\frac{7}{2}$ or $\frac{9}{2}$. J -values and g_J -values have been determined for many of these levels from a study of the longitudinal Zeeman effect in the 5 T (50 kG) field of a superconducting solenoid magnet. The configurations $4f^7 (^8S) 6s 6p$, $4f^7 (^8S) 6s 7p$, $4f^7 (^8S) 5d 6p$ and $4f^6 (^7F) 5d 6s^2$ are discussed in detail. Levels of $4f^6 (^7F) 5d^2 6s$ and $4f^7 (^6I) 6s 6p$ are reported for the first time. Several long series and parts of series have been discovered among the highly excited levels. Some of these can be identified with levels arising from $4f^7 6s (^9S) np$ and $4f^7 6s (^7S) np$ but interpretation is complicated by the presence of several perturbations of unknown origin.

1. INTRODUCTION

Our present knowledge of the electronic energy-level structure of neutral europium is based mainly on the original analysis by Russell & King (1939) who identified the ground level as the level $^8S_{\frac{7}{2}}$ of the configuration $4f^7 6s^2$ and who discovered many configurations built upon the

$4f^7$ (8S) core. Their paper listed numerous levels which they were unable to assign to configurations and Smith & Wilson (1970), by means of a parametric calculation, were able to identify some of these levels as belonging to $4f^6$ (7F) $5d$ $6s^2$. The proximity to a half-filled shell of 4f electrons should result in a somewhat less complex structure than that of most other rare earths, but, despite this advantage, many features of the excited configurations remain unknown. As a contribution towards a better understanding of the structure we have undertaken a detailed investigation of the absorption spectrum in the region 2100–7200 Å†.

Since the ground level, which is of odd parity, is separated by about 1.5 eV from the lowest excited level, an absorption spectrum at moderate temperature consists solely of ground-level transitions and yields directly the positions of even-parity excited levels with $J = \frac{5}{2}, \frac{7}{2}$ or $\frac{9}{2}$. By direct photography we have determined wavelengths and wavenumbers in terms of thorium standards for over 350 absorption lines. The resolution of our spectra has permitted us to determine the larger isotope shifts and to identify those lines with particularly wide hyperfine structure. In addition we have studied the longitudinal Zeeman effect in the 5 T (50 kG) field of a superconducting solenoid magnet. No accurate Zeeman data for the excited levels of the neutral atom were previously available. Our measurements have enabled us to make unambiguous determinations of J -values and g_J -values for over 200 upper levels. This information, as well as providing a critical check on the assignments made by Russell & King (1939), has led to the discovery of many new levels based on both the $4f^6$ and $4f^7$ cores.

Our spectra include the ionization limits defined by the 9S_4 and 7S_3 levels of the configuration $4f^7$ $6s$ in Eu II. A description of the high series members ($n > 40$) converging towards each limit and the autoionization structure between the two limits has already been published (Smith & Tomkins 1975). This paper will be referred to in subsequent sections as I. Hidden within the complex sharp-line spectrum just below the first ionization limit we have discovered at least five series, all of them strongly perturbed. Attempts to establish the connections between these series and the well-defined series at lower principal quantum numbers ($n < 20$) have not yet proved successful.

2. EXPERIMENTAL

Apart from a few visible lines, which we treated separately, the entire sharp-line absorption spectrum lies between 2185 and 3600 Å, and can be photographed at high resolution in a single exposure using the Argonne Laboratory's 9 m (30 ft) concave-grating spectrograph (Tomkins & Fred 1954). A simple absorption furnace, consisting of a stainless-steel tube surrounded by a nichrome heating coil, was placed between the spectrograph slit and a positive-column hydrogen discharge tube providing a background continuum. The furnace, together with a water-cooled jacket, was designed to fit within the cylindrical cavity of a superconducting solenoid magnet capable of producing a 5 T (50 kG) field. Once correctly positioned the furnace was loaded with a few lumps of europium metal and filled to a pressure of 265 Pa (2 Torr) with argon buffer gas. Exposures of the absorption spectrum were made both with and without the magnetic field. Furnace temperatures were varied between 500 and 800 °C so as to cover a wide range of line-strength. In some exposures a Babinet–Soleil compensator and Rochon prism were inserted into the optical train so that the groups of σ^+ and σ^- components could be photographed separately. This separation proved particularly helpful in regions where patterns

† 1 Å = 0.1 nm = 10^{-10} m.

due to neighbouring lines were overlapping. In exposures intended for wavelength measurement the europium spectrum in the second order of a 1200 line/mm grating was photographed alongside a first order comparison spectrum generated by means of an electrodeless thorium lamp. Exposure times of about 60 s on Kodak SWR plates were found to be adequate. The Zeeman patterns of the visible lines were photographed in a separate experiment using a tungsten lamp as background source and 103F or IN plates as appropriate.

Wavelength measurements and reduction to vacuum wavenumbers were made with the semi-automatic photoelectric scanning comparator and data reduction process previously described by Tomkins & Fred (1951, 1963). Thorium wavelengths were taken from Giacchetti, Stanley & Zalubas (1970). All lines used for wavelength measurements were identified on at least two sets of plates, but the final wavelengths are weighted heavily in favour of one set which was judged to be much superior to the others. Best-fit g_J -factors were deduced from measurements on the Zeeman patterns by means of a routine described by Vander Sluis (1956). As a first step all apparently unperturbed patterns were analysed for both upper and lower g_J -factors. By comparing the mean ground-level g_J -factor for each set of exposures with the accurate value of 1.9935 ± 0.0003 determined by Sandars & Woodgate (1960) we obtained a calibration of the magnetic field. The field was found to vary slightly between exposures but was always within the limits 4.80 ± 0.05 T (48.0 ± 0.5 kG). The mean error in the field determination appropriate to a single set of exposures was about 0.02% or 1 mT (10 G). Having calibrated the field we recalculated the upper g_J -factors assuming the ground-level value to be fixed at 1.9935. A small perturbation in a Zeeman pattern could cause a small systematic error in the derived g_J -factor. An estimate of this error, based on the departure of the corresponding ground-level g_J -factor from the mean for a set of exposures, was included in the error quoted for each result.

TABLE 1. LANDÉ g_J -FACTORS FOR THE CONFIGURATION
 $4f^7 ({}^8S) 6s 6p$ IN Eu I

level† cm ⁻¹	term	J	$g_J (LS)‡$	$g_J^{(int)}§$	$g_J^{(exp)} $
14067.79	¹⁰ P	7	2.222	2.200	2.191 (5)
14563.61	¹⁰ P	7	1.960	1.932	1.929 (5)
15890.48	⁸ P	6	2.286	2.234	2.227 (2)
15952.32	⁸ P	6	1.937	1.877	1.875 (2)
16611.81	⁸ P	6	1.778	1.804	1.795 (2)
17340.65	⁶ P	5	1.714	1.798	1.787 (2)
17707.40	⁶ P	5	1.886	1.944	1.94 (1)
21444.59	⁸ P	6	2.286	2.280	2.272 (1)
21605.22	⁸ P	6	1.937	1.934	1.926 (5)
21761.30	⁸ P	6	1.778	1.779	1.773 (2)

† Energy levels are taken from Russell & King (1939).

‡ g_J -factors calculated in LS -coupling.

§ g_J -factors calculated in intermediate coupling: Smith & Wybourne (1965).

|| Measured g_J -factors.

3. RESULTS

In this section we discuss those results which can be directly inferred from measurements on the plates. The interpretation of the energy structure will be considered in §§ 4 and 5. Table 1 contains the measured g_J -values for the upper energy-levels associated with the visible lines: no attempt was made to redetermine the wavelengths of these lines. Results for the ultraviolet

TABLE 2. ABSORPTION SPECTRUM OF EUROPIUM 2212–3600 Å: WAVELENGTHS, INTENSITIES, UPPER LEVELS AND g_J FACTORS

wavelength/Å	intensity	upper level cm ⁻¹	J	g_J	designation
589.260	100 IS	27852.95		2.009 (5)	4f ⁶ (7F) 5d 6s ² 8D
3487.278	10 IS	28667.46		2.194 (1)	4f ⁷ (8S) 5d 6p 10F
3467.871	200	28827.88		1.811 (1)	4f ⁶ (7F) 5d 6s ² 8D
3457.037	300	28918.22		1.841 (2)	4f ⁷ (8S) 5d 6p 10F
3432.513	300 IS	29124.83		1.440 (1)	4f ⁶ (7F) 5d 6s ² 8G
3425.29	1	29186.2		1.70 (3)	4f ⁷ (8S) 5d 6p 10F
3353.698	350 IS	29809.26		1.465 (2)	4f ⁶ (7F) 5d 6s ² 8G
3350.397	500 IS	29838.63		1.676 (1)	4f ⁶ (7F) 5d 6s ² 8D
3334.313	5000	29982.56		2.06 (1)	4f ⁶ (7F) 5d 6s ² 8P
3322.254	1000	30091.39		1.618 (1)	4f ⁶ (7F) 5d 6s ² 8F
3262.482	300	30642.68		1.470 (3)	4f ⁶ (7F) 5d 6s ² 8G
3247.538	1000	30783.67		1.551 (2)	4f ⁶ (7F) 5d 6s ² 8F
3246.011	800	30798.16		P2.14 (1)	4f ⁷ (8S) 5d 6p 8D
	IS	30800.71†		P2.80 (1)	4f ⁷ (8S) 5d 6p 8D
3241.386	800	30842.10		1.824 (3)	4f ⁷ (8S) 5d 6p 8D
3235.108	600 IS	30901.95		1.706 (2)	4f ⁷ (8S) 5d 6p 8D
3230.57	2 IS	30945.4		2.49 (4)	4f ⁷ (8S) 5d 6p 10D
3213.745	2500 IS	31107.36		1.954 (6)	4f ⁶ (7F) 5d 6s ² 6P
3212.804	6000	31116.47		1.928 (5)	4f ⁶ (7F) 5d 6s ² 8P
3210.566	3000	31138.16		2.006 (5)	4f ⁷ (8S) 5d 6p 10D
3203.844	20	31203.49		0.540 (2)	4f ⁶ (7F) 5d ² 6s 10I
3185.552	200 IS	31382.66		1.860 (2)	4f ⁷ (8S) 5d 6p 10D
3168.278	400 IS	31553.76		1.522 (2)	4f ⁶ (7F) 5d 6s ² 8F
3158.296	2	31653.48		0.97 (3)	4f ⁶ (7F) 5d ² 6s 10I
3136.233	2 IS	31876.15		1.719 (2)	4f ⁷ (8S) 5d 6p 8F
3123.770	5 IS	32003.33		1.628 (2)	4f ⁷ (8S) 5d 6p 8F
3111.427	8000	32130.28		1.747 (2)	4f ⁶ (7F) 5d 6s ² 8P
3106.162	1200 IS	32184.73		1.615 (2)	4f ⁷ (8S) 5d 6p 8F
3102.359	20	32224.19		1.17 (1)	4f ⁶ (7F) 5d ² 6s 10I
3085.684	80 IS	32398.32		2.195 (1)	4f ⁷ (8S) 5d 6p 10P
3066.933	400 IS	32596.39		1.93 (1)	4f ⁷ (8S) 5d 6p 10P
3058.975	1000 IS	32681.19		1.729 (1)	4f ⁶ (7F) 5d 6s ² 6P
3032.928	50 IS	32961.85		0.857 (1)	4f ⁶ (7F) 5d 6s ² 6H
3007.018	2	33245.85		1.483 (2)	4f ⁶ (7F) 5d ² 6s
2974.045	2	33614.42		1.479 (2)	4f ⁶ (7F) 5d 6s ² 6D
2959.51	2	33779.50		1.48 (1)	4f ⁶ (7F) 5d ² 6s
2958.885	600 IS	33786.64		2.276 (2)	4f ⁷ (8S) 5d 6p 8P
2950.798	400 WW	33879.23		1.97 (2)	4f ⁷ (8S) 6s 7p 10P
2948.225	200 WW	33908.81		2.180 (2)	4f ⁷ (8S) 6s 7p 10P
2928.417	2	34138.16		1.495 (3)	4f ⁶ (7F) 5d 6s ² 6D
2910.877	2	34343.85		1.32 (2)	4f ⁶ (7F) 5d 6s ² 6F
2908.993	2000 W	34366.09		1.803 (3)	4f ⁷ (8S) 6s 7p 8P
2893.838	500 W	34546.06		1.96 (1)	?4f ⁶ (7F) 5d ² 6s 10P
2893.013	1500 W	34555.91		P2.27 (2)	4f ⁷ (8S) 6s 7p 8P
2892.502	2500 W	34562.01		P1.91 (3)	4f ⁷ (8S) 6s 7p 8P
2878.848	800	34725.92		1.719 (2)	4f ⁷ (8S) 5d 6p 8P
2877.774	400 W	34738.88		1.542 (3)	4f ⁶ (7F) 5d 6s ² 6D
2852.177	25 IS	35050.64		1.394 (4)	4f ⁶ (7F) 5d 6s ² 6F
2807.169	150 W	35612.58		1.716 (3)	4f ⁷ (8S) 6s 7p 6P
2800.000	250 W	35703.76		1.89 (1)	4f ⁷ (8S) 6s 7p 6P
2797.812	50	35731.68		1.458 (1)	4f ⁷ (8S) 5d 6p 6F
2776.512	300	36005.79		2.150 (2)	4f ⁶ (7F) 5d ² 6s 10P
2772.898	200	36052.71		2.202 (1)	8P
2771.435	30	36071.74		1.447 (3)	4f ⁶ (7F) 5d 6s ² 6F
2770.714	10 IS	36081.12		1.462 (2)	4f ⁷ (8S) 5d 6p 6F
2755.153	4 IS	36284.90		1.420 (2)	4f ⁷ (8S) 5d 6p 6F
2747.830	1200	36381.59		1.841 (5)	
2745.609	800	36411.02		P1.624 (5)	
2743.286	1500	36441.86		P2.224 (5)	4f ⁷ (8S) 6s 7p 8P
2738.568	200	36504.63		1.793 (5)	
2735.248	1000	36548.94		1.810 (5)	
2732.598	500	36584.38		P1.971 (5)	4f ⁷ (8S) 5d 6p 8D
	IS	36586.35†		P2.43 (2)	4f ⁷ (8S) 5d 6p 8D
2731.365	600	36600.90		1.91 (1)	
2723.954	2000	36700.46		1.83 (1)	4f ⁷ (8S) 5d 6p 8D

ABSORPTION SPECTRUM OF EUROPIUM

349

TABLE 2 (cont.)

wavelength/Å	intensity	upper level cm ⁻¹	<i>J</i>	<i>g_J</i>	designation
2721.300	15	36736.26		1.103 (1)	4f ⁶ (7F) 5d 6s ² 6G
		36867.04†	1/1	1.662 (3)	4f ⁷ (8S) 5d 6p 8D
2709.981	3000	36889.69		1.729 (2)	4f ⁷ (8S) 5d 6p 8D
2701.778	10	37001.69		1.297 (1)	
2695.062	100	37093.89		1.99 (3)	
2692.719	200 W	37126.16		1.795 (2)	
2690.806	20	37152.55		1.245 (2)	4f ⁶ (7F) 5d 6s ² 6G
2682.582	400 W	37266.44		2.380 (1)	
2680.051	15	37301.64		1.311 (2)	
2665.691	20	37502.57		P	
2665.529	30	37504.85		P	
2659.528	4	37589.48		P1.61 (2)	
2659.398	400	37591.31		P1.58 (2)	
2643.815	200	37812.87		?1.82 (3)	
				?2.17 (3)	
2641.090	50	37851.88		1.65 (1)	
2637.114	100	37908.94		1.375 (1)	4f ⁶ (7F) 5d 6s ² 6G
2631.619	100	37988.09		1.389 (2)	
2625.768	50	38072.73		1.87 (1)	
2625.248	15	38080.28		1.820 (3)	
2619.268	200	38167.22		1.491 (1)	4f ⁷ (8S) 5d 6p 6D
2612.712	20 W	38262.98		1.699 (2)	
2609.822	30	38305.35		1.432 (1)	
2606.052	50 WW	38360.76		1.804 (4)	
2602.581	80	38411.91		1.598 (1)	4f ⁷ (8S) 5d 6p 6D
2591.200	4	38580.62		1.54 (2)	
2584.720	2	38677.34		1.76 (2)	
2580.613	15	38738.88		2.03 (1)	
2568.744	100 W	38917.87		1.796 (2)	4f ⁷ (8S) 5d 6p 6P
2564.962	400 WW	38975.25		1.754 (3)	4f ⁷ 6s (9S) 8p 8P
2562.342	5	39015.09		1.42 (2)	
2561.848	50	39022.63		2.07 (2)	4f ⁷ (8S) 5d 6p 6P
2559.929	5	39051.88		P	4f ⁷ (8S) 5d 6p 8F
2559.407	2	39059.84		P	4f ⁷ (8S) 5d 6p 8F
2554.367	10	39136.89		P	?4f ⁷ (8S) 5d 6p 8F
2551.588	15	39179.52		2.07 (1)	4f ⁷ 6s (9S) 8p 8P
2550.769	2	39192.10		1.70 (1)	
2550.006	1 WW	39203.83		2.16 (2)	4f ⁷ 6s (9S) 8p 10P
2546.587	15 WW	39256.45		1.95 (1)	4f ⁷ 6s (9S) 8p 10P
2541.935	2	39328.30		1.80 (2)	
2523.770	5	39611.35		1.592 (2)	
2513.656	5	39770.72		1.99 (3)	
2512.904	20	39782.62		1.639 (1)	
2494.658	5	40073.57		2.305 (5)	
2484.543	4	40236.71		P	4f ⁷ 6s (7S) 5f 8F
2479.186	200 W	40323.65		1.042 (4)	4f ⁷ (6I) 6s 6p
2476.179	50 W	40372.61		1.58 (1)	
2476.116	500	40373.63		1.436 (1)	
2471.104	1500	40455.51		1.768 (3)	4f ⁷ 6s (7S) 8p 8P
2468.811	10	40493.09		1.529 (3)	
2461.745	1000	40609.30		1.89 (1)	4f ⁷ 6s (7S) 8p 8P
2460.502	800	40629.82		2.264 (2)	4f ⁷ 6s (7S) 8p 8P
2450.693	5	40792.43		1.605 (3)	
2447.649	10 WW	40843.16		1.013 (5)	4f ⁷ (6I) 6s 6p
2446.496	150 W	40862.41		1.692 (2)	4f ⁷ 6s (7S) 8p 6P
2441.897	100 W	40939.36		1.88 (1)	4f ⁷ 6s (7S) 8p 6P
2440.524	400	40962.39		1.64 (2)	
2433.632	5	41078.38		1.149 (2)	
2425.060	500	41223.58		1.708 (4)	
2423.78	2	41245.34		P	
2423.727	20 W	41246.25		P	
2423.632	800	41247.86		P	
2421.569	1500	41283.00		2.256 (5)	4f ⁷ 6s (9S) 9p 8P
2421.418	2000	41285.58		1.762 (5)	4f ⁷ 6s (9S) 9p 8P
2418.483	1000	41335.67		1.775 (1)	
2414.24	2	41408.47		1.609 (5)	
2409.037	5	41497.75		1.357 (3)	
2408.005	150 WW	41515.52		2.210 (5)	4f ⁷ 6s (9S) 9p 10P

TABLE 2 (cont.)

wavelength/Å	intensity	upper level cm ⁻¹	<i>J</i>	<i>g_J</i>	designation
2406.561	250 WW	41540.43		1.97 (1)	4f ⁷ 6s (⁹ S) 9p ¹⁰ P
2403.666	150	41590.46		1.537 (1)	
2401.92	2	41620.68		0.95 (1)	
2401.090	8	41635.08		1.608 (2)	
2397.758	4	41692.92		1.466 (1)	
2394.476	10	41750.07		0.918 (2)	
2389.245	500	41841.47		1.637 (1)	
2386.140	2	41895.92		1.391 (3)	
2385.356	20	41909.69		1.692 (1)	
2383.34	1	41945.18		0.38 (3)	
2379.640	2500	42010.34		1.771 (1)	4f ⁷ (⁸ S) 5d 6p ⁸ P
2377.486	800	42048.40		1.596 (1)	
2375.298	2000	42087.13		1.86 (1)	4f ⁷ (⁸ S) 5d 6p ⁸ P
2372.831	1500	42130.89		2.04 (1)	4f ⁷ (⁸ S) 5d 6p ⁸ P
2372.371	500	42139.06		P 1.4 (1)	
2371.900	400	42147.42		1.642 (2)	
2365.508	300	42261.30		1.583 (1)	
2361.910	10	42325.67		1.463 (1)	
2359.726	150	42364.85		1.232 (5)	4f ⁷ (⁶ I) 6s 6p
2358.078	150	42394.46		1.74 (2)	
2357.565	100	42403.68		0.867 (5)	4f ⁷ (⁶ I) 6s 6p
2352.677	5	42491.77		1.15 (1)	
2352.594	2	42493.27		P	
2352.237	300 W	42499.72		1.657 (2)	
2342.312	5	42679.78		1.517 (1)	
2336.442	3 WW	42787.00		2.210 (3)	4f ⁷ 6s (⁹ S) 10p ¹⁰ P
2335.665	3 WW	42801.24		1.97 (3)	4f ⁷ 6s (⁹ S) 10p ¹⁰ P
2331.065	500 W	42885.69		1.88 (1)	
2329.001	800	42923.70		1.88 (1)	
2328.718	1000 W	42928.91		1.755 (2)	4f ⁷ 6s (⁹ S) 10p ⁸ P
2327.804	600 W	42945.76		1.895 (5)	4f ⁷ 6s (⁹ S) 10p ⁸ P
2327.105	200	42958.67		1.569 (2)	
2326.134	8	42976.60		1.518 (1)	
2320.833	10	43074.75		1.645 (3)	
2316.163	20	43161.59		1.328 (5)	
2315.816	10	43168.06		1.619 (5)	4f ⁷ 6s (⁷ S) 9p ⁶ P
2312.678	30	43226.63		1.620 (2)	
2312.571	60	43228.62		1.84 (1)	4f ⁷ 6s (⁷ S) 9p ⁶ P
2309.645	10	43283.39		1.608 (1)	
2308.678	600	43301.51		2.210 (3)	4f ⁷ 6s (⁷ S) 9p ⁸ P
2307.276	150	43327.82		1.591 (5)	
2307.148	800	43330.23		1.787 (4)	4f ⁷ 6s (⁷ S) 9p ⁸ P
2305.509	5	43361.03		2.05 (1)	
2304.909	400	43372.31		P 1.15 (5)	4f ⁷ (⁶ I) 6s 6p
2304.478	400	43380.42		P 1.15 (5)	4f ⁷ (⁶ I) 6s 6p
2303.855	200	43392.16		1.633 (3)	
2301.912	20	43428.78		P	
2301.413	60	43438.19		1.502 (5)	
2299.214	5	43479.74		1.253 (3)	
2295.002	5 WW	43559.52		2.203 (5)	4f ⁷ 6s (⁹ S) 11p ¹⁰ P
2294.568	100 WW	43567.76		2.0 (1)	4f ⁷ 6s (⁹ S) 11p ¹⁰ P
2292.683	2	43603.59		0.715 (4)	
2291.039	1500 WW	43634.86		P	4f ⁷ 6s (⁹ S) 11p ⁸ P
2290.921	2000 WW	43637.11		P	4f ⁷ 6s (⁹ S) 11p ⁸ P
2289.014	20	43673.46		1.794 (1)	
2287.437	15	43703.57		1.359 (1)	
2285.558	150	43739.50		1.652 (1)	
2284.906	8	43751.97		1.321 (3)	
2280.273	100	43840.86		1.353 (2)	
2277.769	50	43889.05		1.632 (3)	
2274.731	5	43947.66		P	
2274.309	2	43955.82		P	
2270.209	2	44035.19		1.63 (1)	
2269.965	4	44039.93		1.66 (1)	
2268.869	2 WW	44061.21		2.15 (2)	4f ⁷ 6s (⁹ S) 12p ¹⁰ P
2268.42	1 WW	44070.22		1.99 (5)	4f ⁷ 6s (⁹ S) 12p ¹⁰ P
2267.881	150 WW	44080.39		1.96 (2)	4f ⁷ 6s (⁹ S) 12p ⁸ P
2267.279	100 WW	44092.10		2.18 (1)	4f ⁷ 6s (⁹ S) 12p ⁸ P
2267.038	200	44096.79		1.610 (1)	
2263.830	150	44159.26		1.653 (1)	

ABSORPTION SPECTRUM OF EUROPIUM

351

TABLE 2 (cont.)

wavelength/Å	intensity	upper level cm ⁻¹	<i>J</i>	<i>gJ</i>	designation
2263.199	200	44171.58	?	1.616 (2)	
2261.750	50	44199.87	?	1.461 (2)	
2260.385	100	44226.56	?	P	
2259.796	2	44238.08	?	?	
2259.726	2	44239.46	?	?	
2259.470	50	44244.47	?	P	
2254.868	50 W	44334.75	?	P	
2254.761	5	44336.86	?	P	
2252.336	3	44384.60	?	1.118 (2)	
2250.969	2 WW	44411.55	?	2.0 (1)	4f ⁷ 6s (⁹ S) 13p ¹⁰ P
2250.296	5	44424.82	?	P	
2250.255	100 WW	44425.63	?	2.0 (1)	4f ⁷ 6s (⁹ S) 13p ⁸ P
2250.168	150 WW	44427.35	?	2.19 (1)	4f ⁷ 6s (⁹ S) 13p ⁸ P
2248.978	75 W	44450.86	?	1.744 (2)	4f ⁷ 6s (⁷ S) 10p ⁶ P
2247.004	15 W	44489.91	?	P 1.94 (5)	4f ⁷ 6s (⁷ S) 10p ⁶ P
2246.342	200	44503.02	?	1.882 (5)	
2245.029	500	44529.04	?	1.755 (2)	4f ⁷ 6s (⁷ S) 10p ⁸ P
2243.390	150 W	44561.53	?	1.493 (1)	
2242.622	300 W	44576.83	?	2.0 (1)	4f ⁷ 6s (⁷ S) 10p ⁸ P
2241.926	100 W	44590.66	?	P 2.2 (1)	4f ⁷ 6s (⁷ S) 10p ⁸ P
2241.735	40 W	44594.46	?	P 1.67 (1)	
2241.482	20 W	44599.50	?	P 2.0 (1)	
2241.244	200 W	44604.24	?	1.71 (1)	
2240.748	3	44614.11	?	?	
2239.243	150 WW	44644.09	?	1.87 (1)	
2238.730	20	44654.31	?	1.662 (2)	
2238.453	10 WW	44659.84	?	2.0 (1)	4f ⁷ 6s (⁹ S) 14p ¹⁰ P
2237.873	250 WW	44671.42	?	1.786 (5)	4f ⁷ 6s (⁹ S) 14p ⁸ P
2236.52	500 W	44698.5	?	2.20 (1)	4f ⁷ 6s (⁹ S) 14p ⁸ P
2236.52		44698.5	?	1.372 (2)	
2235.289	75	44723.05	?	1.92 (2)	
2234.684	150	44735.16	?	1.81 (1)	
2233.943	100 W	44749.99	?	1.50 (2)	
2232.260	150 W	44783.74	?	1.71 (1)	
2231.759	5	44793.78	?	P	
2231.371	80 W	44801.58	?	P	
2230.198	50 W	44825.13	?	P 2.0 (1)	
2229.271	2 WW	44843.76	?	P	4f ⁷ 6s (⁹ S) 15p ¹⁰ P
2228.869	100 WW	44851.85	?	P	4f ⁷ 6s (⁹ S) 15p ⁸ P
2227.666	150	44876.07	?	1.74 (1)	
2227.098	300	44887.53	?	P 2.28 (2)	4f ⁷ 6s (⁹ S) 15p ⁸ P
2227.027	300 W	44888.96	?	2.0 (1)	4f ⁷ 6s (⁹ S) 15p ⁸ P
2225.348	10	44922.81	?	P	
2224.850	2	44932.85	?	?	
2224.767	30 W	44934.55	?	1.58 (1)	
2223.270	2	44964.80	?	?	
2222.801	20 W	44974.29	?	P 2.0 (1)	
2222.662	2 WW	44977.09	?	?	4f ⁷ 6s (⁹ S) 16p ¹⁰ P
2221.713	75 WW	44996.32	?	P 2.0 (1)	4f ⁷ 6s (⁹ S) 16p ⁸ P
2221.194	150 W	45006.82	?	1.612 (5)	
2220.909	300 WW	45012.59	?	P 2.0 (1)	4f ⁷ 6s (⁹ S) 16p ⁸ P
2220.290	100	45025.15	?	1.752 (5)	
2218.450	1	45062.51	?	?	
2218.390	1	45063.73	?	?	
2217.200	5 W	45087.89	?	?	4f ⁷ 6s (⁹ S) 17p ¹⁰ P
2216.643	1 W	45099.21	?	?	4f ⁷ 6s (⁹ S) 14 f ⁸ F
2216.269	100 WW	45106.83	?	P 2.0 (1)	4f ⁷ 6s (⁹ S) 17p ⁸ P
2216.059	150 WW	45111.10	?	P 2.0 (1)	4f ⁷ 6s (⁹ S) 17p ⁸ P
2215.798	100	45116.42	?	1.58 (1)	
2215.574	5	45120.98	?	1.70 (5)	
2213.915	1	45154.80	?	?	
2213.840	3	45156.32	?	?	
2213.252	8 W	45168.30	?	?	4f ⁷ 6s (⁹ S) 18p ¹⁰ P
2212.670	1 W	45180.18	?	?	4f ⁷ 6s (⁹ S) 18p ¹⁰ P
2212.404	1	45185.63	?	?	4f ⁷ 6s (⁹ S) 15 f ⁸ F
2212.305	50 WW	45187.63	?	?	4f ⁷ 6s (⁹ S) 18p ⁸ P
2212.218	75 WW	45189.42	?	?	4f ⁷ 6s (⁹ S) 18p ⁸ P
2212.129	100 WW	45191.23	?	?	4f ⁷ 6s (⁹ S) 18p ⁸ P

† Wavenumbers taken from Russell & King (1939).

TABLE 3. ABSORPTION SPECTRUM OF EUROPIUM 2189–2212 Å: WAVELENGTHS, INTENSITIES, UPPER ENERGY LEVELS AND EFFECTIVE QUANTUM NUMBERS

wavelength/Å	intensity	upper level cm ⁻¹	n*	series	comments
2211.418	2 W	45205.78	14.401		
2210.393	2	45226.72	14.695	Y	sharp
2209.891	2	45237.00	14.845		sharp
2209.767	1 W	45239.54	14.883		
2209.456	2 W	45245.91	14.980		
2209.220	25 WW	45250.73	15.055		
2209.181	25 WW	45251.54	15.067		
2208.962	20	45256.02	15.138	Z	
2208.829	100	45258.76	15.181		
2208.768	110 WW	45260.00	15.201		4f ⁷ 6s (⁹ S) 19p
2208.649	50 W	45262.44	15.238		
2206.886	80 W	45298.60	15.859		
2206.730	1	45301.79	15.917		
2206.665	2 W	45303.14	15.942		
2206.578	110 W	45304.93	15.975		4f ⁷ 6s (⁷ S) 11p
2206.551	20	45305.47	15.985		
2206.420	10 W	45308.18	16.036		
2206.169	1	45313.31	16.133	Z	
2206.096	2	45314.82	16.162	Z	
2205.786	150 WW	45321.20	16.286		4f ⁷ 6s (⁹ S) 20p
2204.982	110 W	45337.71	16.621		
2204.879	150 W	45339.82	16.666		
2204.515	1	45347.29	16.825		
2204.290	2 WW	45351.93	16.927		
2204.107	2 WW	45355.70	17.011		
2203.830	1	45361.40	17.140	Z	
2203.686	50 WW	45364.35	17.208		4f ⁷ 6s (⁹ S) 21p
2203.532	150 WW	45367.53	17.283		4f ⁷ 6s (⁹ S) 21p
2202.833	3	45381.92	17.631		sharp
2202.555	3 W	45387.66	17.777		
2202.301	4 WW	45392.89	17.912		
2202.186	6 WW	45395.27	17.975		
2201.913	1	45400.87	18.125	Z	
2201.801	120 WW	45403.19	18.188		two lines
2201.570	80 W	45407.95	18.320		
2200.948	150 WW	45420.78	18.690	A'	
2200.816	50 W	45423.50	18.772	B'	
2200.719	2	45425.52	18.833		sharp
2200.629	50 WW	45427.36	18.889	C'	
2200.572	8 WW	45428.55	18.926	D'	
2200.540	10 WW	45429.20	18.946	D'	
2200.259	2 WW	45435.01	19.129		
2200.184	2 WW	45436.57	19.178		
2199.656	500 W	45447.46	19.538	A' B'	
2199.209	75 W	45456.70	19.860	C'	
2199.118	2 W	45458.58	19.928	D'	? two lines
2198.943	1	45462.21	20.060		fairly sharp
2198.882	1	45463.45	20.105		
2198.746	3 W	45466.28	20.211		
2198.572	250 WW	45469.87	20.348	A'	
2198.484	120 W	45471.70	20.418	B'	
2197.987	75 W	45481.97	20.829	C'	
2197.890	1	45483.98	20.912	D'	? two lines
2197.565	200 WW	45490.70	21.198	A'	
2197.464	100 W	45492.79	21.289	B'	
2197.071	1	45500.93	21.656	E'	fairly sharp

ABSORPTION SPECTRUM OF EUROPIUM

353

TABLE 3 (cont.)

wavelength/Å	intensity	upper level cm ⁻¹	n*	series	comments
2196.937	10 W	45503.70	21.785	C'	
2196.864	2	45505.22	21.857		
2196.820	1	45506.12	21.900		
2196.741	4 W	45507.76	21.979		
2196.637	75 WW	45509.92	22.084	A'	
2196.565	1	45511.41	22.158		
2196.264	2	45517.64	22.473		
2196.065	2	45521.77	22.690	C'	E' fairly sharp
2195.886	1	45525.49	22.891	D	
2195.801	1	45527.25	22.987		
2195.531	3	45532.84	23.301		E' sharp
2195.449	2	45534.55	23.402		
2195.393	1	45535.70	23.471		
2195.079	3 W	45542.22	23.864	D	
2194.950	1	45544.90	24.031	A	
2194.820	10 W	45547.59	24.203		E
2194.722	2	45549.63	24.336	C	
2194.385	6 W	45556.61	24.808		D
2194.242	4 WW	45559.59	25.018	A	
2194.198	1	45560.51	25.084	B	
2194.142	1	45561.66	25.167		E
2194.057	1	45563.42	25.296	C	
2193.802	4 W	45568.72	25.696		D
2193.620	4 WW	45572.50	25.993	A	blend
2193.459	2	45575.84	26.265	C	
2193.298	1	45579.19	26.546	D	
2193.125	1	45582.78	26.857		F
2193.070	10 WW	45583.93	26.959	A	blend
2192.918	1	45587.09	27.246	C	
2192.632	1	45593.04	27.811		F
2192.593	150 W	45593.85	27.891	A	
2192.537	1	45595.01	28.006	B	
2192.442	1	45597.00	28.208	C	
2192.205	200 W	45601.92	28.724	A	
2192.105	3	45604.00	28.952	B	
2191.989	1	45606.41	29.221		D
2191.926	120 W	45607.71	29.371	A	
2191.867	100 W	45608.95	29.515		?F
2191.713	1	45612.15	29.897	B	
2191.603	8	45614.44	30.179		D blend
2191.384	2	45619.00	30.768	B	fairly sharp
2191.314	1	45620.47	30.96		diffuse
2191.242	1	45621.95	31.17	A	D blend
2191.175	2	45623.35	31.36	B	
2190.98	1	45627.41	31.95		diffuse
2190.92	1	45628.59	32.12		diffuse
2190.88	1	45629.54	32.27	B	diffuse
2190.68	1	45633.62	32.91		diffuse
2190.60	1	45635.41	33.21	B	diffuse
2190.38	1	45639.99	34.00		diffuse
2190.11	1	45645.51	35.03		diffuse
2189.90	1	45650.27	36.00		diffuse
2189.65	1	45654.57	36.96		diffuse

lines are contained in tables 2 and 3, a division being made at 2212 Å. Because of increasing line-density no useful Zeeman data can be deduced for lines shortward of this wavelength. However, it turns out that most of the high-lying levels can be fitted into series converging towards the first ionization limit ($45\,734.92\text{ cm}^{-1}$). In table 3 we therefore include the effective quantum number (n^*) of each level with respect to this limit.

(a) *Wavelengths, intensities and upper energy levels*

In the first three columns of tables 2 and 3 are listed the wavelength in standard air, an estimate of the intensity and the vacuum wavenumber of every absorption line we could discover between 3600 and 2189 Å (the spectrum between 2189 and 2100 Å was described in I). Since every line is a transition from the ground level each vacuum wavenumber also determines the position of an upper energy-level. Comparisons between measurements on different plates suggest that wavelengths should be accurate to better than 0.005 Å and wavenumbers to better than 0.05 cm^{-1} , apart from a few extremely weak lines whose values are quoted to lower accuracy. Our measurements are superior in accuracy to the emission measurements of King (1938) but we note that there is good agreement between the two lists for wavelengths down to 2365 Å. At shorter wavelengths there are no obvious coincidences between our own lines and the earlier list, which extends down to 2109 Å. It seems either that the ground-level transitions did not occur with sufficient intensity in King's light-source or that his results contain a systematic wavelength error below 2365 Å. The reliability of our own wavelength scale is confirmed by measurements on several impurity lines (e.g. Zn I, 2138.57 Å) which yield wavelengths in good agreement with previously accepted values.

Intensity estimates are based on photoelectric measurements of plate transmission at peak absorption. They correspond roughly to a scale of absorption oscillator strength in which the strongest resonance line (4594 Å) has strength 100 000. Absolute accuracy is probably no better than order of magnitude since the plates were not calibrated for intensity measurement and no account was taken of differences in line-width. Many transitions to the lower excited levels (below $37\,000\text{ cm}^{-1}$) showed a large isotope shift (see part (c) of this section) and these lines are denoted by IS following the intensity. Other transitions throughout the spectrum showed obvious hyperfine structure: these are denoted by W (moderate h.f.s.) and WW (wide h.f.s.). Lines with wide hyperfine structure invariably showed a characteristic pattern in which the strongest component belonging to the isotope with the larger nuclear moment appeared as a satellite on the short-wavelength side of the main zero-field line (see figure 5*a*, plate 1).

(b) *J-values and g_J -values*

For the majority of lines, J -values and g_J -values could be determined unambiguously from the observed Zeeman patterns. The results are listed in tables 1 and 2. The figure in brackets following the g_J -value denotes the estimated error in the last decimal place quoted. Levels with $g_J = 2.0 \pm 0.1$ give rise to unresolved Zeeman patterns and consequent difficulties in the determination of J . All uncertain J -values must, however, be $\frac{5}{2}$, $\frac{7}{2}$, or $\frac{9}{2}$. As the density of lines increases towards the series limit the Zeeman patterns become increasingly more perturbed and difficult to interpret. In the region $2200 < \lambda < 2220\text{ Å}$ some lines show the asymmetric Zeeman splitting characteristic of the quadratic Zeeman effect. These lines are clearly associated with high series members but none of the patterns are sufficiently well-defined to justify detailed measurement. At longer wavelengths there are isolated examples of close lines whose

ABSORPTION SPECTRUM OF EUROPIUM

355

patterns are distorted by mutual perturbation of the upper levels. When these perturbations are not too severe the g_J -values can still be derived by means of a fairly simple analysis based on second order perturbation theory. In cases of severe perturbation the Zeeman patterns become unrecognizable. The presence of perturbations is indicated by a letter P in the fifth column of table 2, and two interesting examples are shown in figures 5*c* and *d*, plate 1.

In an effort to discover the uncertain J -values we have searched the list of unclassified emission lines (King 1938) for transitions between our new upper levels and the low-lying odd levels arising from $4f^7$ (8S) $5d$ $6s$. This approach proved fruitless. With the exception of a few levels associated with the 8P multiplets at about 40 600 and 42 100 cm^{-1} , levels above 40 000 cm^{-1} in our list do not appear to contribute significantly to the emission spectrum.

TABLE 4. ISOTOPE SHIFTS IN EU I

level/ cm^{-1}	$4f^7$ (8S) $5d$ $6p$ designation	i.s./ cm^{-1}	level/ cm^{-1}	$4f^6$ (7F) $5d$ $6s^2$ designation	i.s./ cm^{-1}
28667.46	$^{10}F_{7/2}^{8S}$	-0.250	27852.95	$^8D_{3/2}^{7F}$	+0.203
30800.71	$^8D_{3/2}^{8S}$	-0.250	29124.83	$^8G_{7/2}^{7F}$	+0.212
30901.95	$^8D_{5/2}^{8S}$	-0.255	29809.26	$^8G_{9/2}^{7F}$	+0.207
30945.38	$^{10}D_{3/2}^{8S}$	-0.242	29838.63	$^8D_{5/2}^{8S}$	+0.210
31382.66	$^{10}D_{5/2}^{8S}$	-0.244	31107.36	$^6P_{7/2}^{8S}$	+0.170
31876.15	$^8F_{7/2}^{8S}$	-0.262	31553.76	$^8F_{7/2}^{8S}$	+0.194
32003.33	$^8F_{9/2}^{8S}$	-0.255	32681.19	$^6P_{9/2}^{8S}$	+0.140
32184.73	$^8F_{5/2}^{8S}$	-0.172	32961.85	$^6H_{7/2}^{8S}$	+0.177
32398.32	$^{10}P_{7/2}^{8S}$	-0.204	35050.64	$^6F_{7/2}^{8S}$	+0.160
32596.39	$^{10}P_{9/2}^{8S}$	-0.185			
33786.64	$^8P_{3/2}^{8S}$	-0.160			
35731.68	$^6F_{5/2}^{8S}$	-0.130			
36081.12	$^6F_{7/2}^{8S}$	-0.248			
36284.90	$^6F_{9/2}^{8S}$	-0.237			
36586.35	$^8D_{5/2}^{8S}$	-0.192			

error in i.s. $\approx 0.010 \text{ cm}^{-1}$.

(c) Isotope shifts

Natural europium consists of two isotopes, ^{151}Eu and ^{153}Eu , with almost equal abundances. The resolution of our spectra was such that isotope shifts $\gtrsim 0.1 \text{ cm}^{-1}$ were easily measurable. Lines showing a large isotope shift are denoted by IS following the intensity in table 2 and the corresponding measurements are listed in table 4. In discussing these we shall anticipate some of our conclusions concerning configuration assignments which are described in the next section. Large isotope shifts appear to be associated with transitions from the ground level to levels of just two configurations, $4f^7$ (8S) $5d$ $6p$ and $4f^6$ (7F) $5d$ $6s^2$, but not all transitions to these configurations show large shifts. Although the equal abundances of the two isotopes make it impossible for us to determine the sign of the shift, there is clear evidence that the shifts are reduced by mixing and must therefore be of opposite sign. There seems little doubt that the signs are the same as those observed in similar transitions in other rare earths (e.g. Sm I, Striganov, Katulin & Eliseev 1962) and appropriate signs have been incorporated into table 4. Despite the spread of values there is an apparent clustering about the shifts of -0.250 and $+0.200 \text{ cm}^{-1}$ for transitions to $4f^7$ (8S) $5d$ $6p$ and $4f^6$ (7F) $5d$ $6s^2$ respectively. These values must approximately represent the shifts of the pure configurations relative to $4f^7$ (8S) $6s^2$. Figure 5*b*, plate 1 shows an example of a transition with large isotope shift.

Transitions to levels of other configurations show no obvious evidence of isotope shift though-

in the case of $4f^7$ (8S) $6s$ n p configurations, any isotope shift is likely to be masked by hyperfine structure. Transitions to $4f^6$ (7F) $5d^2$ $6s$ are particularly sharp indicating approximately zero shift with respect to the ground level. The total disappearance of isotope shifts in transitions to levels higher than $36\,600\text{ cm}^{-1}$ suggests that configuration mixing is appreciable among the more highly excited levels.

4. CONFIGURATION STRUCTURE

With the extensive new data on J -values and g_J -values we can now attempt to assign the energy-levels to configurations. The large spread of g_J -values throughout table 2 suggests that the concept of configurations retains some validity even as high as $45\,000\text{ cm}^{-1}$ above the ground level. In this section we shall consider those configurations based on both the $4f^6$ and $4f^7$ cores which can reasonably be treated individually. Consideration of the long series arising mainly from an excited p-electron will be deferred until the next section. Configuration assignments which can be made with some degree of confidence are given in the final column of table 2. For levels below $40\,000\text{ cm}^{-1}$ it is usually possible to give a term as well as a configuration assignment, though the use of LS -coupling labels is not intended to imply that a pure coupling scheme is entirely appropriate. Levels based on the $4f^6$ core are particularly strongly mixed. In comparing our conclusions with those of Russell & King (1939) we emphasize again that our results only concern levels with $J = \frac{5}{2}, \frac{7}{2}$ or $\frac{9}{2}$.

(a) $4f^7$ (8S) $6s$ $6p$

The levels of this configuration were identified by Russell & King (1939). In table 1 we compare our measured g_J -values with theoretical values calculated in LS -coupling and in intermediate coupling (Smith & Wybourne 1965). In every case there is excellent agreement between the measurement and the intermediate-coupling calculation.

(b) $4f^7$ (8S) $5d$ $6p$

Russell & King (1939) claimed to have discovered all the levels of this configuration but their identification of the higher 8P term was questioned by Smith & Wybourne (1965) on theoretical grounds. Our present results support the conclusion of Smith & Collins (1970) who, on the evidence of a low-resolution absorption spectrum, placed this term at about $42\,000\text{ cm}^{-1}$. This problem will be further discussed in the context of the long 8P series. We can confirm all the other assignments made by Russell & King apart from the levels $^8P_{\frac{3}{2}}$, $^6D_{\frac{3}{2}}$ and $^8F_{\frac{3}{2}}$ at $34\,102$, $38\,457$ and $39\,086\text{ cm}^{-1}$ respectively. No trace of any lines connected with these levels can be found on our plates. The absence of transitions to the last two levels is not surprising since the multiplets to which they belong are only weakly connected with the ground level. The absence of a transition to $34\,102\text{ cm}^{-1}$ is, however, very puzzling since Russell & King found good evidence for this level based on strong transitions to the low-lying 8D terms of $4f^7$ (8S) $5d$ $6s$. In addition, the $J = \frac{5}{2}$ and $J = \frac{9}{2}$ members of the 8P multiplet are easily identifiable at $33\,786$ and $34\,726\text{ cm}^{-1}$ by means of their relatively strong transitions to the ground level. Only two levels with unresolved Zeeman patterns (compatible with $^8P_{\frac{7}{2}}$) contribute to the absorption spectrum in the region of $34\,102\text{ cm}^{-1}$. These are less favourably placed, at $33\,879$ and $34\,546\text{ cm}^{-1}$, with respect to the other members of the 8P multiplet and evidence to be presented in (c) below suggests an alternative interpretation. We can only assume that the level

at $34\,102\text{ cm}^{-1}$ is real and that its proximity to an ${}^8\text{P}_{\frac{3}{2}}$ level of $4f^7\text{ (}^8\text{S) }6s\,7p$ has produced an unusual cancellation in the transition probability to the ground level.

Agreement between the measured g_J -values and the intermediate-coupling calculation of Smith & Wybourne (1965) is not as impressive as in (a) above but the difference between observed and calculated values is less than 0.1 in every case except one. The exception is the ${}^6\text{P}_{\frac{3}{2}}$ level at $39\,022\text{ cm}^{-1}$ which appears to be strongly mixed with another $J = \frac{5}{2}$ level at $39\,179\text{ cm}^{-1}$. Transitions to the higher ${}^8\text{F}$ term are very weak and the Zeeman patterns are extremely perturbed. This is compatible with the original analysis which discovered several levels in close proximity.

(c) $4f^7\text{ (}^8\text{S) }6s\,7p$

This configuration is sufficiently low-lying to be treated separately but identification of its levels raises many problems. Several of the assignments suggested by Russell & King (1939) are unacceptable on theoretical grounds. We expect to find four multiplets: ${}^{10}\text{P}$, ${}^8\text{P}$, ${}^6\text{P}$ and ${}^8\text{P}$ in order of increasing energy. By means of our Zeeman data we can immediately identify two ${}^6\text{P}$ levels, at $35\,612$ and $35\,703\text{ cm}^{-1}$, and the three levels of the lower ${}^8\text{P}$ term at $34\,366$, $34\,556$ and $34\,562\text{ cm}^{-1}$. The perturbation of the latter multiplet can be explained by the fact that it lies within a much wider ${}^8\text{P}$ multiplet arising from $4f^7\text{ (}^8\text{S) }5d\,6p$. The higher ${}^8\text{P}$ multiplet of $4f^7\text{ (}^8\text{S) }6s\,7p$ is presumably to be found among the group of levels at about $36\,500\text{ cm}^{-1}$ all of which combine strongly with the ground level. A diagonalization of the $f^7\text{ (}^8\text{S) }sp$ energy matrices with appropriate radial parameters predicts that the ${}^{10}\text{P}$ term should be a normal multiplet centred at about $34\,000\text{ cm}^{-1}$ and with a total spread of about 300 cm^{-1} . The level at $33\,908\text{ cm}^{-1}$ has the appropriate J - and g_J -values for ${}^{10}\text{P}_{\frac{3}{2}}$ and is much better placed than the level at $36\,005\text{ cm}^{-1}$ suggested by Russell & King. On the other hand, Russell & King's identification of a level at $34\,317\text{ cm}^{-1}$ with ${}^{10}\text{P}_{\frac{1}{2}}$ is quite compatible with theory. There is no $J = \frac{9}{2}$ level between $33\,908$ and $34\,317\text{ cm}^{-1}$ but a likely candidate for the missing ${}^{10}\text{P}$ occurs at $33\,879\text{ cm}^{-1}$. The associated absorption line has wide hyperfine structure, similar to that observed in the transition to $33\,908\text{ cm}^{-1}$, and an unresolved Zeeman pattern compatible with either ${}^{10}\text{P}_{\frac{3}{2}}$ or ${}^8\text{P}_{\frac{3}{2}}$. There remains the problem of the level at $34\,546\text{ cm}^{-1}$ identified by Russell & King as ${}^{10}\text{P}_{\frac{3}{2}}$: this also gives rise to an unresolved Zeeman pattern but has only moderate hyperfine structure. We believe this to be a $J = \frac{9}{2}$ level originating from $4f^6\text{ (}^7\text{F) }5d^2\,6s$. Its presence could explain why the true ${}^{10}\text{P}_{\frac{3}{2}}$ ($33\,879\text{ cm}^{-1}$) is perturbed to below its expected position.

(d) $4f^6\text{ (}^7\text{F) }5d\,6s^2$

Smith & Wilson (1970), by means of a parametric calculation, were able to identify many of the octet levels of this configuration among the levels discovered by Russell & King in the region $27\,500$ – $33\,000\text{ cm}^{-1}$. On the evidence of our Zeeman data we can confirm all these identifications and in addition we can suggest likely identifications for most of the sextet levels. With one exception the ${}^8\text{H}$ and ${}^6\text{H}$ levels do not contribute significantly to the absorption spectrum. The exception is ${}^6\text{H}_{\frac{3}{2}}$ which presumably is able to make an observable transition to the ground level because of its proximity to ${}^6\text{P}_{\frac{3}{2}}$. A thorough search of our plates for the missing transitions has revealed two extremely weak lines corresponding to levels at $25\,066.9$ and $32\,371.1\text{ cm}^{-1}$. We were unable to obtain Zeeman patterns for these but the first is probably an ${}^8\text{H}$ level and the second may be ${}^6\text{H}_{\frac{3}{2}}$. Figure 1 illustrates the structure deduced for this configuration: unobserved levels (distinguished by broken lines) are drawn in the positions

predicted by Smith & Wilson (1970). Substantial departures from LS -coupling are indicated by the observed structure and confirmed by the g_J -values listed in table 2.

(e) $4f^6 ({}^7F) 5d^2 6s$

No levels of this configuration had been discovered prior to the present investigation but Brewer (1971) had predicted from thermodynamic data that the lowest levels should occur at about $30\,000\text{ cm}^{-1}$. On our plates we find evidence for three levels, at $31\,203$, $31\,653$ and $32\,224\text{ cm}^{-1}$, whose g_J -values are close to those expected for a ${}^{10}I$ term. Only $4f^6 5d^2 6s$ can provide such a term in this energy region. Four other levels below $36\,050\text{ cm}^{-1}$ do not fit into the configurations described in (a)–(d) above. We presume that these, at $33\,245$, $33\,779$, $34\,546$ and $36\,005\text{ cm}^{-1}$, must also originate from $4f^6 5d^2 6s$. On the evidence of their g_J -values and of their transitions to $4f^7 ({}^8S) 5d 6s$ the last two appear to have ${}^{10}P$ character. Russell & King assigned them to $4f^7 ({}^8S) 6s 7p$ but in (c) above we have given reasons for rejecting these particular assignments. Dr J-F. Wyart of the Laboratoire Aimé Cotton, Orsay, France has kindly undertaken a preliminary calculation of $4f^6 ({}^7F) 5d^2 6s$. This suggests that there are many more levels below $36\,000\text{ cm}^{-1}$ than we have discovered and that the lowest levels might belong to a ${}^{10}G$ rather than a ${}^{10}I$ term. We conclude that levels of this configuration only contribute to the absorption spectrum when they happen to interact strongly with nearby levels to which transitions are more probable. It is nevertheless surprising that the ${}^{10}I$ levels, which one would expect to be particularly pure, should give rise to easily observable lines.

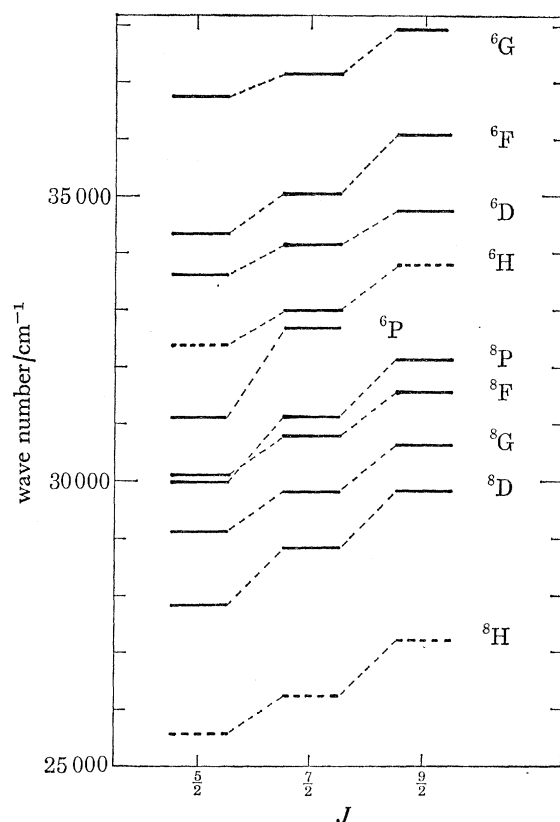


FIGURE 1. Structure of levels with $J = \frac{5}{2}, \frac{7}{2}$ and $\frac{9}{2}$ in the configuration $4f^6 ({}^7F) 5d^2 6s^2$. Levels not yet discovered are denoted by broken lines and plotted in positions predicted by theory.

(f) $4f^6 ({}^7F) 5d^3$

According to Brewer (1971) levels of this configuration should commence at about $43\,000\text{ cm}^{-1}$. Several levels with low g_J -values in this region may belong to $4f^6 ({}^7F) 5d^3$ but could equally well originate from $4f^7 ({}^6I) 6s 6p$.

(g) Levels based on excited parent terms of $4f^7$

The excited terms of $4f^7$ occur in the order 6P , 6I , 6D with increasing energy. In Eu III the separation between the 6P and 6I terms is about 3500 cm^{-1} (Sugar & Spector 1974). Our spectra contain several moderately strong transitions to levels above $40\,000\text{ cm}^{-1}$ with unusually low g_J -values. These levels must surely originate from $4f^7 ({}^6I) 6s 6p$ and the most obvious of them are identified in the last column of table 2. It seems likely that levels based on the 6P parent will occur below $40\,000\text{ cm}^{-1}$, perhaps even as low as $36\,500\text{ cm}^{-1}$. In the region of $43\,000\text{ cm}^{-1}$ there are several levels with g_J -values of about 1.6 which again are associated with moderately strong absorption lines: these levels are probably the lowest arising from the 6D parent. Until we have some idea of the detailed structure of configurations built on excited terms of $4f^7$ we are unable to make further progress.

5. LONG SERIES

The absorption spectrum should contain long series arising from successive excitations of a p-electron. The series may be divided into four main channels: ${}^{10}P$ and 8P channels converging towards the $4f^7 6s, {}^9S_4$ ground level of Eu II together with 8P and 6P channels converging towards the $4f^7 6s {}^7S_3$ limit only 1669 cm^{-1} higher. From measurements on high series members ($n > 40$) these limits have been determined to be $45\,734.9$ and $47\,404.1\text{ cm}^{-1}$ (see I for details).

Levels of the ${}^{10}P$ channel as far as $n = 15$ (principal quantum number of the excited p-electron) were relatively easy to identify by means of the Zeeman data. Table 5 lists the levels together with their effective quantum numbers (n^*), g_J -values and the estimated intensities of the corresponding absorption lines. All the levels have wide hyperfine structure. The decimal part of the effective quantum number is remarkably constant in this region showing that there are no significant perturbations of the series. Through lack of intensity the series cannot be followed beyond $n = 15$ but it is likely that ${}^{10}P$ levels reappear among the perturbed series to be described later.

Levels of the 6P channel are shown in table 6. The identifications are reasonably certain as far as $n = 10$ although the quantum defects ($n - n^*$) are not as constant as in the previous case. Possible identifications for the $n = 11$ and $n = 12$ levels are shown in brackets. Effective quantum numbers are the only available evidence in this region. Our proposed identifications for the $n = 12$ levels correspond to the two broad features in the absorption spectrum at about 2187 \AA just in front of the first ionization limit (see figure 3). Although there is no 6P continuum immediately beyond this limit it is possible that 6P levels just below the limit might derive additional width through spin-orbit interaction with the strongly autoionized $n = 12$ 8P levels.

The two 8P channels constitute a major problem. Although strong lines appear in approximately the positions indicated by a quantum defect analysis, there are very few regular multiplets. In some cases the appearance of two lines rather than three may simply be due to blending but it is clear that most multiplets are extremely perturbed. If the problem was simply

one of two interacting channels converging towards different limits, it should be amenable to a graphical analysis of the type described by Lu & Fano (1970). Investigations along these lines have, however, proved unsuccessful indicating the presence of perturbations external to the two main channels. The progress of the lower series members in both channels can be followed with reasonable certainty. Levels which can definitely be identified with ^8P multiplets are noted in table 2 and the progress of the two channels is illustrated in figure 2 (a representative effective quantum number is plotted for each multiplet). Both channels appear to suffer a major perturbation in the region of $42\,000\text{ cm}^{-1}$. The levels at $42\,010$, $42\,087$ and $42\,130\text{ cm}^{-1}$ form an obvious ^8P multiplet whose effective quantum numbers with respect to the two limits (5.45 and 4.53 respectively) do not fit easily into either of the $6s\text{ }np$ channels. This multiplet is the only one above $40\,000\text{ cm}^{-1}$ (apart from the ^8P at $40\,600\text{ cm}^{-1}$ which falls more nearly into the $6s\text{ }np$ sequence) to make transitions of appreciable intensity to the low-lying ^8D terms of $4f^7(^8\text{S})\text{ }5d\text{ }6s$. We therefore identify the perturbing multiplet with the high-lying ^8P term of $4f^7(^8\text{S})\text{ }5d\text{ }6p$ (see § 3(b)) in agreement with Smith & Collins (1970).

TABLE 5. RYDBERG SERIES IN EU I: $4f^7\text{ }6s(^9\text{S})\text{ }np$, ^{10}P (LIMIT: $45\,734.92\text{ cm}^{-1}$)

n	level/ cm^{-1}	J	n^*	g_J	int	
6	14 067.79	7	1.861	2.191	360	
	14 563.61		1.876	1.929	930	
7	33 908.81		3.046	2.180	500	
8	—		—	—	—	—
	39 204.0		4.099	—	—	1
9	39 256.45		—	4.116	1.95	45
	41 515.52		5.100	—	2.210	350
10	41 540.43		—	5.115	1.97	560
	42 787.00		6.101	—	2.210	1
11	42 801.24		—	6.116	2.00	2
	43 559.52		7.102	—	2.203	1
12	43 567.76		—	7.116	2.0	380
	44 061.21		8.097	—	2.150	1
13	44 070.22		—	8.119	1.99	1
	44 411.55		—	9.106	—	1
14	44 659.84	—	10.103	—	3	
15	44 843.61	—	11.106	—	1	

TABLE 6. RYDBERG SERIES IN EU I: $4f^7\text{ }6s(^7\text{S})\text{ }np$, ^6P (LIMIT: $47\,404.13\text{ cm}^{-1}$) †

n	level/ cm^{-1}	J	n^*	g_J	int	
6	17 340.65	7	1.911	1.787	970	
	17 707.40		1.922	1.94	780	
7	35 612.58		3.051	1.716	450	
8	35 703.76		—	3.063	1.89	350
	40 862.41		4.096	—	1.692	630
9	40 939.36		—	4.120	1.88	500
	43 168.06		5.090	—	1.619	40
10	43 228.62		—	5.127	1.84	320
	44 450.86		6.096	—	1.744	55
11	44 489.91		—	6.136	1.94	15
	(45 205.78)		—	7.066	—	2
12	(45 239.54)		—	7.121	—	1
	(45 697)		—	8.02	—	10
	(45 713)		—	8.06	—	5

† Doubtful assignments are enclosed in brackets.

ABSORPTION SPECTRUM OF EUROPIUM

361

The (^9S) np , ^8P and (^7S) np , ^8P channels, although suffering other smaller perturbations in addition to the major perturbation described above, may be followed as far as $n = 18$ and $n = 11$ respectively. The $n = 12$ levels of the second channel probably lie beyond the first ionization limit and, together with subsequent series members, form the basis for the distinctive auto-ionization features described in I. Beyond $n = 18$ the first channel suffers such severe perturbations that, apart from perhaps $n = 19$ and $n = 20$, it no longer makes sense to label levels in

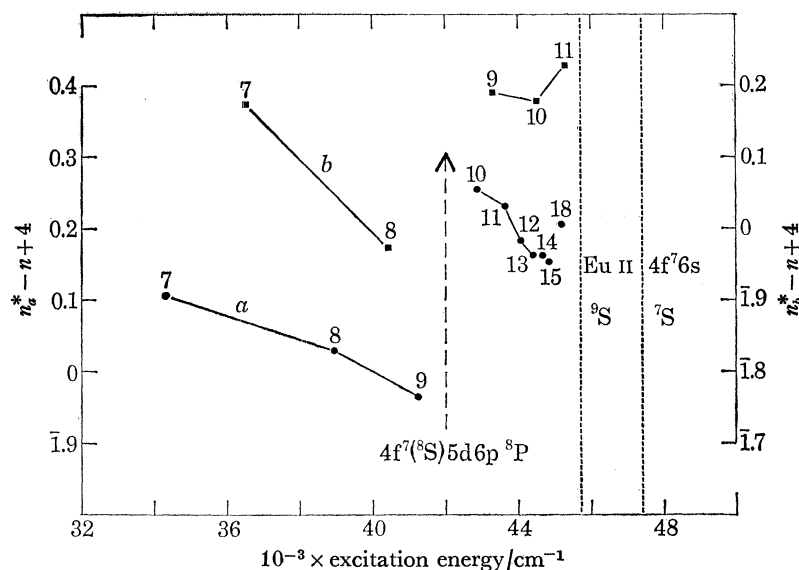


FIGURE 2. Effective quantum number (n^*) plot for lower members of the two ^8P channels (a and b) arising from $4f^7 6s$ (^9S) np and $4f^7 6s$ (^7S) np respectively. Each point is labelled with the appropriate value of the principal quantum number (n).

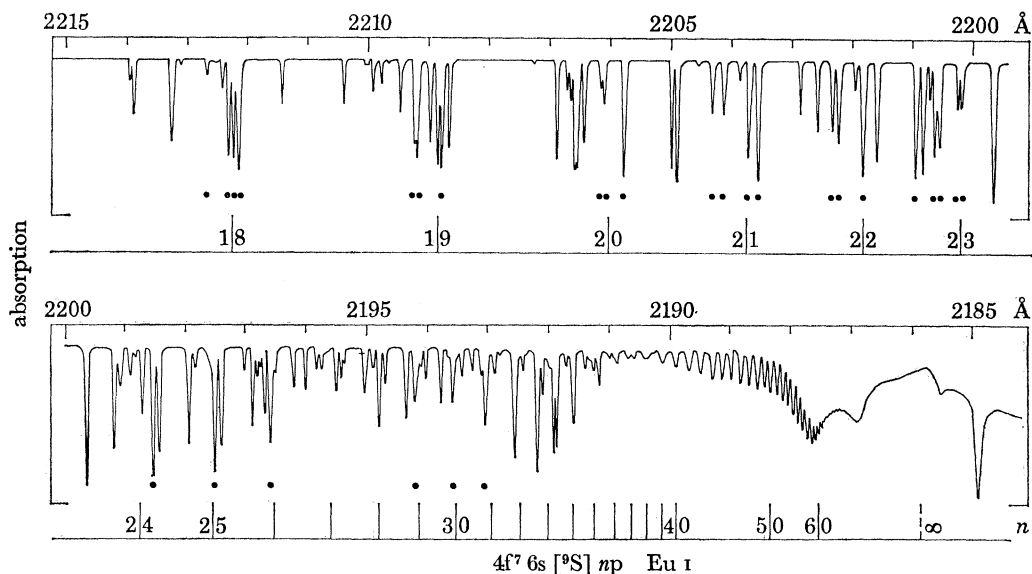


FIGURE 3. Photoelectric scan of the europium absorption spectrum between 2215 and 2185 Å. Filled circles indicate lines with wide hyperfine structure. Positions predicted for unperturbed members of the ^8P channel arising from $4f^7 6s$ (^9S) np are marked below the scan and labelled with the appropriate principal quantum number (n).

an 8P sequence. The situation is illustrated in figure 3 which shows a photoelectric scan covering the last 30 Å prior to the ionization limit. One might hope to see regular triplets of lines converging towards the limit but there is only one obvious triplet – at 2212 Å ($n = 18$). This triplet shows the 10:8:6 intensity ratios characteristic of transitions to an unperturbed 8P term, thus enabling J -values to be assigned. Taking this triplet to define the quantum defect for unperturbed terms we have marked on figure 3 the positions predicted for other channel members as far as $n = 40$. Clusters of strong lines occur close to these predicted positions but there are more lines than one would expect and no obvious multiplets. Many of the lines (those marked with filled circles in figure 3) show the wide hyperfine structure which seems to be characteristic of levels built upon $4f^7 6s, ^9S$. No lines in this region produce recognizable Zeeman patterns so further interpretation must depend on a careful study of effective quantum numbers.

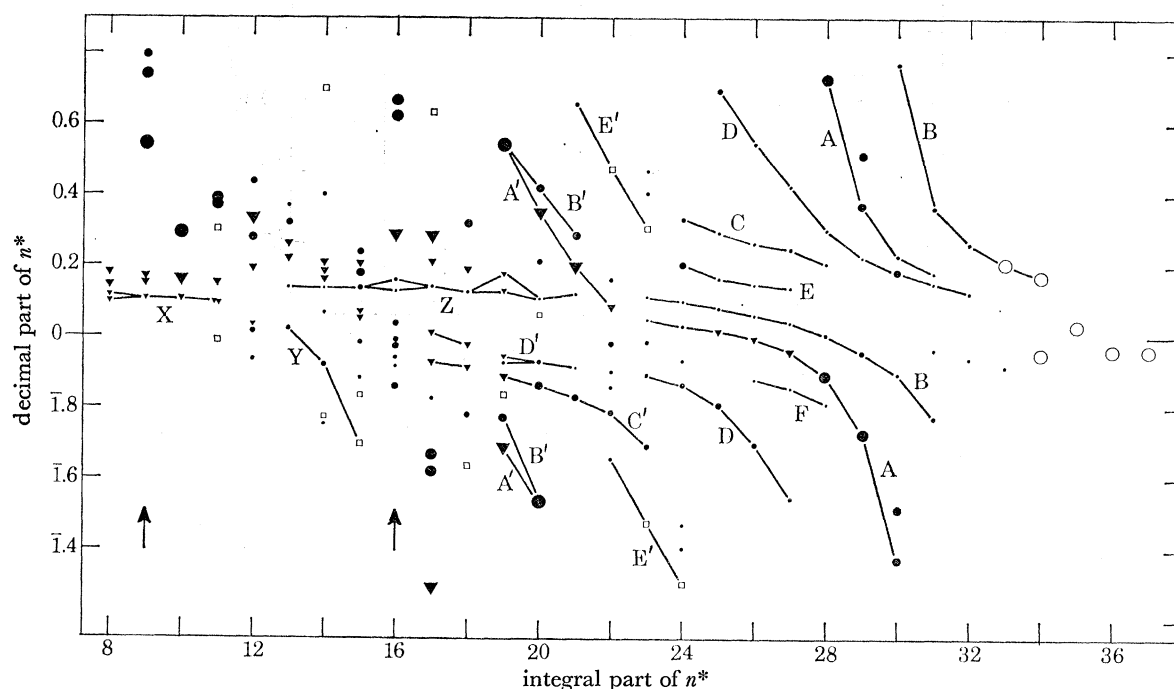


FIGURE 4. Effective quantum number (n^*) plot for levels near the first ionization limit in europium. Links are drawn between those levels which clearly belong to series. Arrows indicate the regions occupied by the $n = 10$ and $n = 11$ multiplets arising from $4f^7 6s (^7S) np$. Key: \blacktriangledown , levels with wide hyperfine structure; \bullet , levels with moderate h.f.s.; \square , relatively sharp levels; \circ , diffuse levels. The size of each symbol (apart from those representing diffuse levels) indicates roughly the strength of the associated absorption line. Note that some symbols well away from the main channels (ordinate *ca.* 0.2) are plotted both at the top and at the bottom of the figure with a change of one unit in x - and y -coordinates.

In table 3 we list the effective quantum numbers, with respect to the first ionization limit, of all levels between $45\,200\text{ cm}^{-1}$ ($n^* \approx 14$) and $45\,655\text{ cm}^{-1}$ ($n^* \approx 37$) which can definitely be established from the absorption spectrum. The levels are displayed in figure 4 where we have plotted the decimal part of each effective quantum number ($n^* - n + 4$ for p-levels) against the corresponding integral part ($n - 4$). Any point in figure 4 can easily be identified with a level in table 3 by combining x - and y -coordinates in the form $x + y$ to give the full effective quantum number. In the figure we have used different symbols to distinguish levels which appear sharp from those with moderate or wide hyperfine structure. The size of each

filled circle or triangle gives a rough indication of the strength of the associated absorption line. A few levels have been included both at the top and at the bottom of the figure (with the appropriate change of one unit in x - and y -coordinates) so as to illustrate their relation to other levels more clearly. Levels which appear sharp (open squares) are unlikely to be part of the basic series structure but may be associated with perturbations. The diffuse levels on the right hand side of the figure merge into the single long series which was described in detail in I. The associated absorption lines can be seen extending to beyond $n = 60$ in figure 3. On the left hand side of figure 4 the main channel of (^9S) np , ^8P levels is represented by the sequence of heavy triangular symbols proceeding roughly parallel to the x -axis at an ordinate of about 0.2. Arrows at $n^* = 9$ and $n^* = 16$ indicate the regions occupied by the $n = 10$ and $n = 11$ members of the (^7S) np , ^8P channel. An excess of levels associated with strong absorption lines is evident in these regions and at $n^* = 16$ the main channel suffers a perturbation. Since the $n = 12$ members of the second ^8P channel probably lie beyond the ionization limit, any other perturbations in the region covered by figure 4 must have some other explanation.

A likely source of further perturbations is the configuration $4f^7$ (^8S) $5d$ $7p$ whose lower levels are believed to occur in the region of the first ionization limit. Among these will be both ^{10}P and ^8P levels which can interact with the corresponding series converging towards this limit. Parr (1971) identified two strong resonances in his photoionization spectrum with the $^8\text{P}_{\frac{3}{2}}$ and $^8\text{P}_{\frac{1}{2}}$ levels of $4f^7$ (^8S) $5d$ $7p$. These features are clearly present in our absorption spectrum at 2184.9 \AA (see figure 3) and 2166.5 \AA (see figure 1 of I). We agree that these features must arise from ^8P levels but can find no strong evidence for the particular choice of J -values. We have estimated appropriate radial parameters for $4f^7$ (^8S) $5d$ $7p$ and calculated the approximate energy structure by diagonalizing the combined electrostatic and spin-orbit matrices. Our calculation slightly favours the association of the two above features with $^8\text{P}_{\frac{3}{2}}$ and $^8\text{P}_{\frac{1}{2}}$ respectively. The alternative interpretation suggested by Parr cannot, however, be ruled out and this would imply the presence of an $^8\text{P}_{\frac{3}{2}}$ level at $45\,450 \pm 100 \text{ cm}^{-1}$. In either case we predict $^{10}\text{P}_{\frac{3}{2}}$ and $^{10}\text{P}_{\frac{1}{2}}$ levels at $45\,300 \pm 150 \text{ cm}^{-1}$ and $45\,600 \pm 150 \text{ cm}^{-1}$ respectively.

In figure 4 we have drawn links between those levels which appear to fall into series. In establishing these links we have sought both a well-defined sequence of n^* values and similarity in appearance of the associated absorption lines. On the right of the figure almost all the levels can be arranged into five, or possibly six, series (labelled A–F). Series F is rather poorly defined but may be connected with the level at $n^* = 29.5$ which would otherwise be isolated. The five main series can be traced backwards through at least one perturbation. There is an intensity minimum in the region of $n^* = 23$ and although further series, labelled A'–E', can be discerned to the left of here it is not obvious how these relate to the first group. It seems likely that A' and A are connected since many levels in both series have wide hyperfine structure and are associated with strong absorption lines. The connections C' to C and E' to E also appear logical. Series B, however, might be related either to B' or to the weak series Z. Similarly D' might be related either to D or to F. Series X on the left hand side of the figure is the end of the unperturbed ^{10}P channel listed in table 5. Slightly to the right of the point where series X disappears is a short series (labelled Y) culminating in a sharp level at $n^* = 14.70$ ($45\,226 \text{ cm}^{-1}$). Series Y cannot be an ^8P series since a complete ^8P multiplet is present at $n^* \approx 14.2$. Series Y must therefore be a ^{10}P series and seems likely to be $^{10}\text{P}_{\frac{3}{2}}$. If we identify the perturbing level at $45\,226 \text{ cm}^{-1}$ as $^{10}\text{P}_{\frac{3}{2}}$ of $4f^7$ (^8S) $5d$ $7p$ we should expect, on the basis of our calculation, to find the corresponding $^{10}\text{P}_{\frac{3}{2}}$ at about $45\,500 \text{ cm}^{-1}$. This could explain the perturbation in either C'

or E' at $n^* \approx 24$. Series Y probably reappears as series D' but this cannot be confirmed without knowledge of J -values. The only other obvious series in the central region of figure 4 is a series (labelled Z) associated with very weak absorption lines and with relatively constant quantum defect (ordinate ≈ 0.14). This can only be the series (9S) nf , 8F which is likely to appear at high principal quantum numbers because of l -mixing. This series will be perturbed by the 8F levels of $4f^7$ (8S) $5d$ $7p$ which, according to our calculation, lie in the region $45\,600 \pm 200$ cm^{-1} .

The central region of figure 4 between $n^* = 16$ and $n^* = 19$ is extremely confused. The spectrum is dominated by pairs of strong lines, one line of each pair having wide hyperfine structure and the other having only moderate hyperfine structure. The corresponding levels form series A' and B'. The level at $45\,447$ cm^{-1} fits into this sequence and must therefore be double. This would explain why the associated absorption line is much the strongest in this part of the spectrum. The strength of the lines associated with series A' and B' indicates that these series must originate from 8P levels and must somehow join the main 8P channel at an ordinate of 0.2. The nature of this connection remains obscure, as does the origin of the perturbations at $n^* \approx 19$. Neither can we offer any explanation for the perturbations in A, B and D at $n^* \approx 30$. It is tempting to identify our five main channels with the five ^{10}P and 8P levels which can make transitions to the $J = \frac{7}{2}$ ground level. However, we cannot rule out the possibility that one or two of the weaker series might involve f-electrons rather than p-electrons. The assignment of the levels to the different series is given in table 3. We emphasize that, apart from the levels marked sharp, even those levels without a label must in some way yet to be determined fit into the series structure.

6. CONCLUSION

A high-resolution study of the europium absorption spectrum has yielded extensive information about the energy structure of even-parity excited levels. J -values and g_J -values have been determined for many of these levels by means of the longitudinal Zeeman effect. Although only levels with $J = \frac{5}{2}$, $\frac{7}{2}$ or $\frac{9}{2}$ are accessible from the ground level, a knowledge of these is sufficient to give a much clearer picture of the configuration structure than was hitherto available. All levels below $36\,000$ cm^{-1} which contribute to the absorption spectrum can be assigned to configurations, and, where intermediate-coupling calculations are available, there is good agreement between calculated and measured g_J -values. Levels of $4f^6$ (7F) $5d^2$ $6s$ have been identified for the first time but not in sufficient quantity to determine the detailed structure within this configuration. At higher energies the analysis is complicated by the presence of levels based on excited terms of the $4f^7$ core. Levels arising from $4f^7$ (6I) have been identified but again there is insufficient information to determine the detailed structure. The wide range of g_J -values revealed by the present experiment suggests that, even among levels of fairly high excitation, further progress with a theoretical interpretation in terms of separate configurations might be possible.

The absorption spectrum also provides us with an opportunity to study the long series converging towards the first and second ionization limits. Series of the type $4f^7$ $6s$ (9S) np and $4f^7$ $6s$ (9S) nf have been discovered converging towards the first limit and $4f^7$ $6s$ (7S) np converging towards the second. The five series arising from $4f^7$ $6s$ (9S) np are of particular interest. For $n \leq 18$ they may be divided into ^{10}P and 8P channels though minor perturbations of the latter channel often make it impossible to identify all three levels comprising the 8P multiplet.

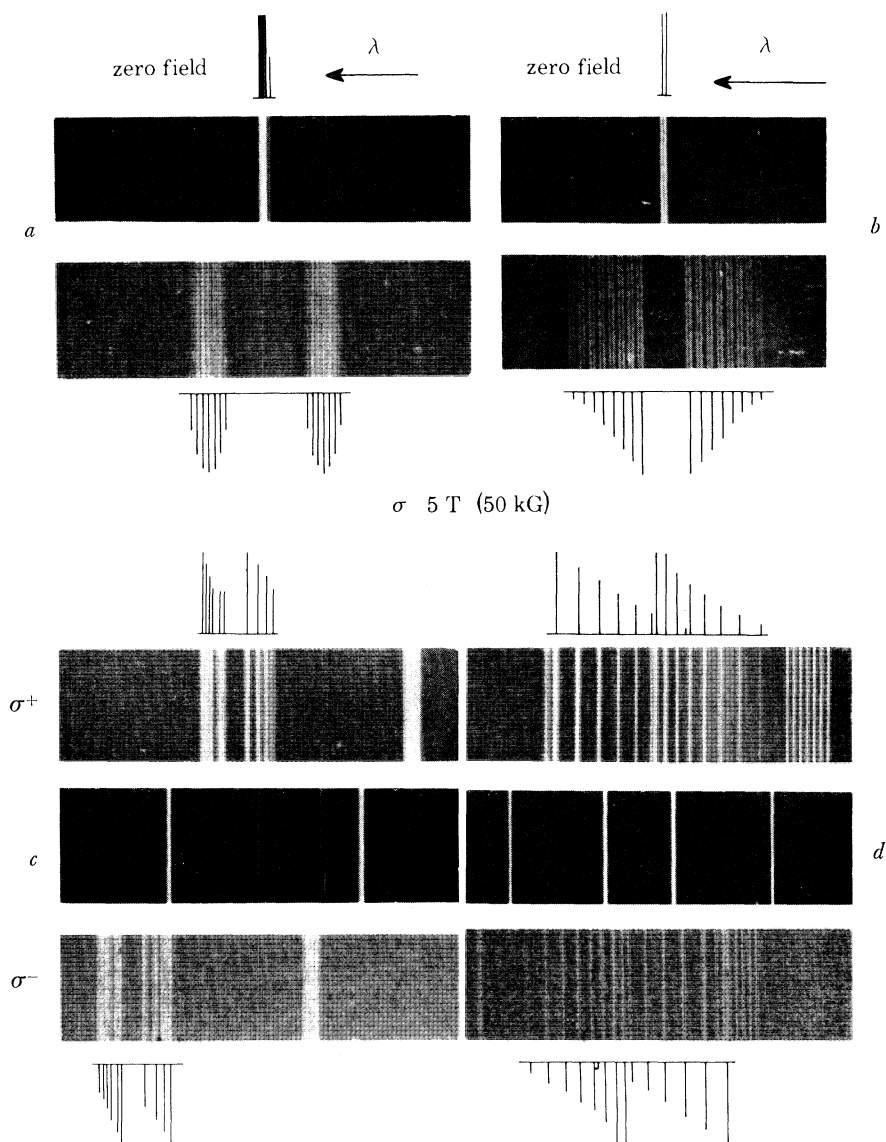


FIGURE 5. Examples of the longitudinal Zeeman effect at a field of 5 T (50 kG) in the absorption spectrum of europium. All transitions are from the $J = \frac{7}{2}$ ground level ($g_J = 1.9935$).

(a) 2948.22 Å: transition to a $J = \frac{7}{2}$ upper level ($g_J = 2.18$) with hyperfine structure typical of a $4f^7 6s (^8S) np$ series member.

(b) 3235.11 Å: transition to a $J = \frac{9}{2}$ upper level ($g_J = 1.71$) with large isotope shift.

(c) 2732.60/2731.36 Å: transition on the left is to a $J = \frac{5}{2}$ upper level ($g_J = 1.97$). Adjacent to this is a $J = \frac{3}{2}$ level to which transitions are normally forbidden. In the presence of the field, there is mutual perturbation between corresponding magnetic sub-levels and four additional components appear in each σ -group. In the absence of the perturbation the transition to the $J = \frac{5}{2}$ level would appear like the typical unresolved pattern on the right.

(d) 2304.91/.48 Å: the transitions in the centre are to two mutually perturbing $J = \frac{9}{2}$ levels with equal g_J -values (1.15). Note that the Zeeman pattern is symmetrical about a point mid-way between the two zero-field lines. The advantage of separating σ^+ from σ^- is evident in this case. The right hand transition is to a $J = \frac{7}{2}$ upper level and the left hand transition has an unresolved pattern.

Between $n = 18$ and $n = 40$ all five series suffer such severe perturbations that they cannot be followed continuously. The origins of most of these perturbations remain unknown. Lack of knowledge of J -values and the presence of additional series arising from excited f-electrons complicates the analysis. If a few J -values could be determined, perhaps from measurements of hyperfine splittings, for the isolated sections of series discovered at $n > 23$, it should be possible to relate these sections to the main channels. The nature of the perturbing levels is likely to remain a mystery, however, since they have largely been assimilated into the existing series and will not therefore have any properties by which they may be distinguished.

An early set of plates, which helped to stimulate this project, was measured at Imperial College, University of London, and we should like to express our grateful thanks to Professor W. R. S. Garton, F.R.S. and Mr J. E. G. Wheaton for help and hospitality received while visiting their laboratory. Mr B. Ercoli of the Argonne National Laboratory rendered invaluable assistance with the construction and operation of the apparatus used in this investigation. We are also indebted to Dr J. F. Wyart of the Laboratoire Aimé Cotton, Orsay, France, who undertook a theoretical calculation on our behalf which helped to clarify our interpretation of the spectrum. One of us (G.S.) gratefully acknowledges financial support, for his visit to Argonne, from Oxford University, the Royal Society of London and the National Bureau of Standards, Washington D.C. This work was supported in part by the U.S. Atomic Energy Commission.

REFERENCES

- Brewer, L. 1971 *J. opt. Soc. Am.* **61**, 1101.
 Giacchetti, A., Stanley, R. W. & Zalubas, R. 1970 *J. opt. Soc. Am.* **69**, 474.
 King, A. S. 1938 *Astrophys. J.* **89**, 377.
 Lu, K. T. & Fano, U. 1970 *Phys. Rev.* **A2**, 81.
 Parr, A. C. 1971 *J. chem. Phys.* **54**, 3161.
 Russell, H. N. & King, A. S. 1939 *Astrophys. J.* **90**, 155.
 Sandars, P. G. H. & Woodgate, G. K. 1960 *Proc. R. Soc. Lond. A* **257**, 269.
 Smith, G. & Collins, B. S. 1970 *J. opt. Soc. Am.* **60**, 866.
 Smith, G. & Tomkins, F. S. 1975 *Proc. R. Soc. Lond. A* **342**, 149.
 Smith, G. & Wilson, M. 1970 *J. opt. Soc. Am.* **60**, 1527.
 Smith, G. & Wybourne, B. G. 1965 *J. opt. Soc. Am.* **55**, 121.
 Striganov, A. R., Katulin, V. & Eliseev, V. V. 1962 *Opt. & Spectrosc.* **12**, 91.
 Sugar, J. & Spector, N. 1974 *J. opt. Soc. Am.* **64**, 1484.
 Tomkins, F. S. & Fred, M. 1951 *J. opt. Soc. Am.* **41**, 641.
 Tomkins, F. S. & Fred, M. 1954 *Spectrochim. Acta* **6**, 139.
 Tomkins, F. S. & Fred, M. 1963 *Appl. Optics* **2**, 715.
 Vander Sluis, K. L. 1956 *J. opt. Soc. Am.* **46**, 605.

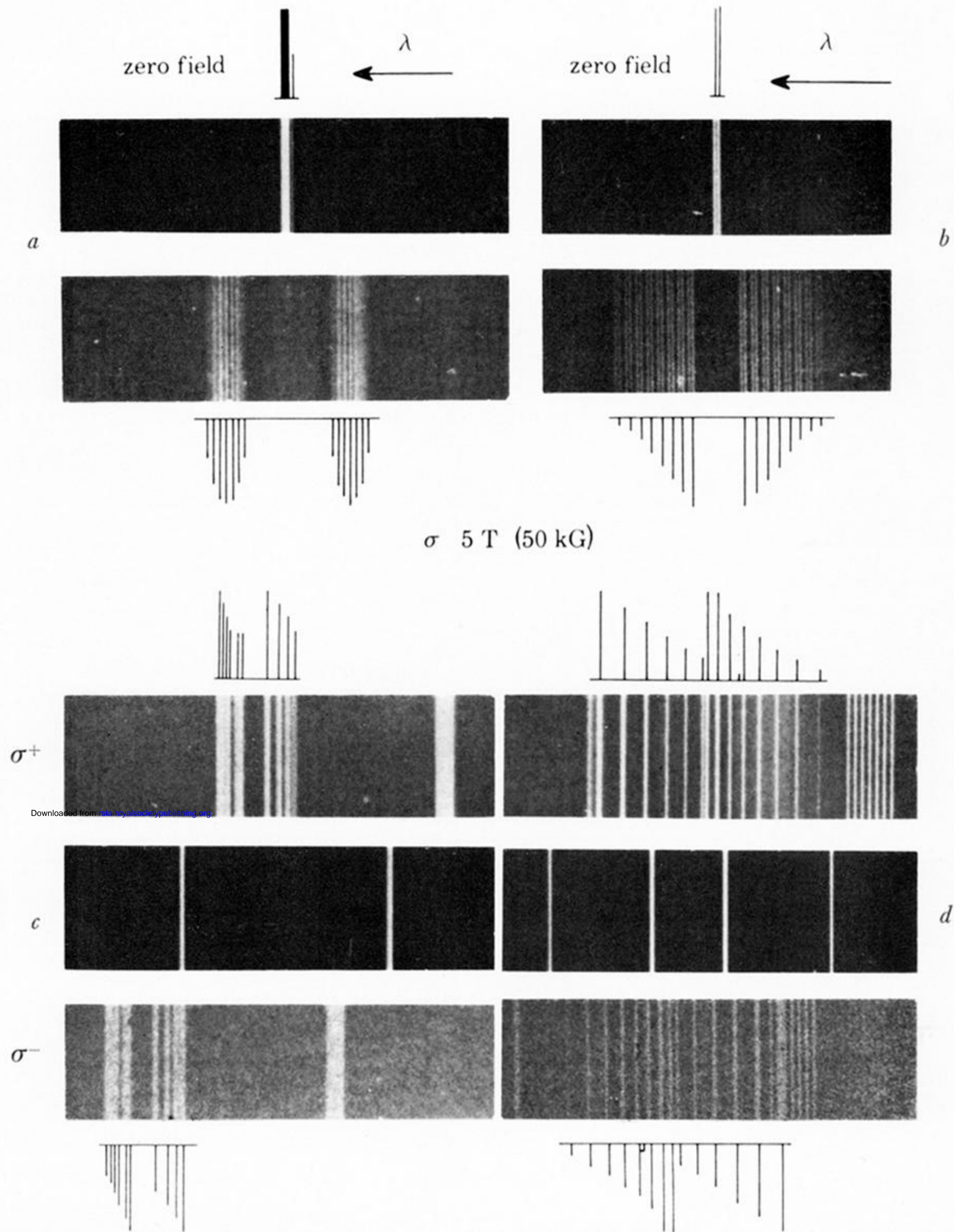


FIGURE 5. Examples of the longitudinal Zeeman effect at a field of 5 T (50 kG) in the absorption spectrum of europium. All transitions are from the $J = \frac{7}{2}$ ground level ($g_J = 1.9935$).

(a) 2948.22 Å: transition to a $J = \frac{7}{2}$ upper level ($g_J = 2.18$) with hyperfine structure typical of a $4f^7 6s$ (9S) np series member.

(b) 3235.11 Å: transition to a $J = \frac{9}{2}$ upper level ($g_J = 1.71$) with large isotope shift.

(c) 2732.60/2731.36 Å: transition on the left is to a $J = \frac{5}{2}$ upper level ($g_J = 1.97$). Adjacent to this is a $J = \frac{3}{2}$ level to which transitions are normally forbidden. In the presence of the field, there is mutual perturbation between corresponding magnetic sub-levels and four additional components appear in each σ -group. In the absence of the perturbation the transition to the $J = \frac{5}{2}$ level would appear like the typical unresolved pattern on the right.

(d) 2304.91/.48 Å: the transitions in the centre are to two mutually perturbing $J = \frac{9}{2}$ levels with equal g_J -values (1.15). Note that the Zeeman pattern is symmetrical about a point mid-way between the two zero-field lines. The advantage of separating σ^+ from σ^- is evident in this case. The right hand transition is to a $J = \frac{7}{2}$ upper level and the left hand transition has an unresolved pattern.